THE JOURNAL OF PHYSICAL CHEMISTRY B

Article

pubs.acs.org/JPCB

Kinetics and Thermodynamics of 1-Hydroxyethyl Radical Reaction with Unsaturated Lipids and Prenylflavonoids

Natália E. C. de Almeida, Inara de Aguiar, Andressa de Zawadzki, and Daniel R. Cardoso*

Instituto de Química de São Carlos, Universidade de São Paulo, Avenida Trabalhador São-Carlense 400, CEP 13560-970 São Carlos, SP, Brazil

Supporting Information

ABSTRACT: Hydroxyalkyl radicals have been reported to induce lipid oxidation as the key aspect of the pathogenesis of alcoholic fatty liver disease and are responsible for the alkylation and cleavage of DNA during the metabolism of a wide range of genotoxic compounds. However, relevant kinetic data for the oxidation of unsaturated lipids by 1-hydroxyethyl radical (HER) has not been reported. In this study, the rate constants for the reaction of unsaturated fatty acid methyl esters and sterols with HER have been determined using a competitive kinetic approach employing the spin-trap α-(4-pyridyl-1-oxide)-*N*-*tert*-butylnitrone (4-POBN) as the competitive substrate. Polyunsaturated fatty acid methyl ester is shown to react with HER with an apparent second-order rate constant ranging from $(3.7 \pm 0.1) \times 10^6$ L mol^{-1} s^{-1} for methyl linoleate to $(2.7 \pm 0.2) \times 10^7$ L mol^{-1} s^{-1} for methyl docosahexanoate at 25.0 ± 0.2 °C in ethanol. The apparent second-order rate constant for polyunsaturated fatty acid methyl ester oxidation by HER is dependent on the number of bisallylic hydrogen atoms rather than on the bond dissociation energy value for the weakest C—H bond as determined by ab initio density functional theory calculations. Sterols displayed higher reactivity compared to unsaturated fatty acid methyl esters with apparent second-order rate constants of $(2.7 \pm 0.1) \times 10^6$ and $(5.2 \pm 0.1) \times 10^7$ L mol^{-1} s^{-1} at 25.0 ± 0.2 °C in ethanol for cholesterol and ergosterol, respectively. Similar experiments with prenylflavonoids as potential herbal chemopreventive agents for preventing alcoholic liver diseases yield apparent second-order rate constants close to the diffusion control with k_{app} values of (1.5 ± 0.2) and $(3.6 \pm 0.1) \times 10^9$ L mol^{-1} s^{-1} for 6-prenylnarigerin and xanthohumol at 25.0 ± 0.2 °C in ethanol solution, respectively. Polyunsaturated lipids were revealed to be highly reactive oxidizable substrates toward HER-induced oxidation in biological systems leading to damage of membranes and sensitive structures.

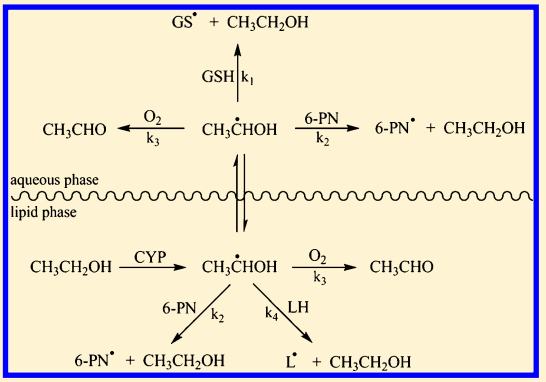

1. INTRODUCTION

Oxidative stress may be defined as the production of reactive redox species that exceeds the detoxifying ability of a living organism. The natural antioxidant defense system comprises antioxidant enzymes (e.g., superoxide dismutase and catalase) and endogenous nonenzymatic metabolites like glutathione (GSH). Under oxidative stress, a shift in living organism redox homeostasis takes place, leading to damage of biomolecules, sensitive structures, and DNA. Carbon-centered radicals, like hydroxyalkyl radicals, have been shown to induce thiol-containing peptides and protein oxidation, to induce DNA cleavage, and to alkylate purine and pyrimidine bases.[1−7]

Ethanol is well-known to be toxic to various biological systems.[1−3] The toxicity of ethanol in living organisms is primarily attributed to radical metabolites formed during its metabolism in the liver.[1−4] Ethanol is known to promote hepatotoxicity through the involvement of 1-hydroxyethyl radical (HER), leading to depletion of cellular antioxidants like GSH and to subsequent liver damage.[4−7]

Phenolic compounds, such as plant secondary metabolites, are ubiquitous in the plant kingdom with a structural diversity that is considered virtually infinite. Recent epidemiologic studies have demonstrated that the consumption of plant-rich meals may induce beneficial health effects.[8] Prenylflavonoids (Figure 1) have attracted considerable attention relating to their biological functions, including a hepatoprotective effect in tetrachloride-induced acute liver injury.[9] Prenylflavonoids possess an isoprenoid unit in the diphenylpropane structure that has been shown to enhance cellular uptake, tissue accumulation, and biological function.[10]

With this in mind, we report herein on the kinetic and thermodynamic capacity of dietary plant phenolic compounds, especially prenylflavonoids, to inhibit lipid peroxidation induced by 1-hydroxyethyl radical, which may lead to maintenance of hepatic redox homeostasis and protect sensitive structures in vivo against oxidative damage.

2. MATERIALS AND METHODS

Chemicals and Materials. Acetonitrile, ethanol, and methanol were obtained from Panreac (Barcelona, Spain). Ferric

Received: September 9, 2014
Revised: November 19, 2014
Published: November 19, 2014

   dx.doi.org/10.1021/jp509125b | J. Phys. Chem. B 2014, 118, 14278−14287

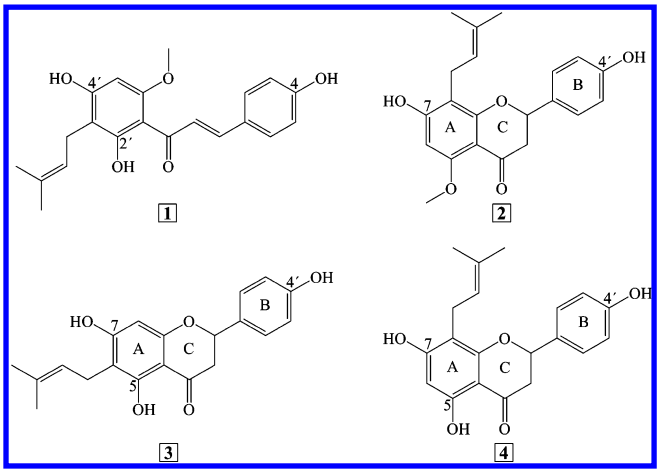

Figure 1. Chemical structures of xanthohumol (XN, **1**), isoxanthohumol (IXN, **2**), 6-prenylnaringenin (6-PN, **3**), and 8-prenylnaringenin (8-PN, **4**).

chloride tetrahydrate ($FeCl_2{\cdot}4H_2O$) and 30% hydrogen peroxide were purchased from Merck (Darmstadt, Germany). Cinnamaldehyde, cholesterol, methyl ester of conjugated (9*E*,11*E*)-linoleic acid (CLA, C18:2 9*E*,11*E*), methyl ester of docosahexaenoic acid (DHA, C22:6), ferrocene, formic acid, isoxanthohumol (IXN), methyl ester of linoleic acid (C18:2), methyl ester of linolenic acid (C18:3), methyl ester of arachidonic acid (C20:4), methyl ester of oleic acid (C18:1), 6-prenylnaringenin (6-PN), 8-prenylnaringenin (8-PN), α-(4-pyridyl-1-oxide)-*N*-*tert*-butylnitrone (4-POBN), tetrabutylammonium perchlorate, and xanthohumol (XN) were obtained from Sigma-Aldrich (Steinheim, Germany). Water was purified (18 MΩ cm) by means of a Milli-Q purification system from Millipore (Bedford, MA, U.S.). Argon (purity grade 99.999%) was purchased from White Martins (Sertãozinho, São Paulo, Brazil). All solvents were of HPLC grade and used without further purification.

Formation of HER and Competitive Kinetics Studies. The formation of HER and the respective spin-trapping reaction employing 4-POBN were conducted at 25.0 ± 0.2 °C through the reaction initiated by adding 80 μL of H_2O_2 (59.0×10^{-3} mol L^{-1}) in an ethanol solution containing 1 mL of 4-POBN solution (3.2×10^{-3} mol L^{-1}) and 60 μL of $FeCl_2{\cdot}4H_2O$ aqueous solution at pH 4.5 (2.0×10^{-3} mol L^{-1}) after exhaustive purging with high-purity argon. The competitive kinetics approach was assayed by monitoring the spin adduct HER/4-POBN by electron paramagnetic resonance (EPR) spectroscopy following the procedure previously reported by de Almeida et al.[11] In this way, the reactions were carried out as described above employing varying concentrations of substrate prenylflavonoids and unsaturated fatty acid methyl esters and sterols (Figures 1 and 2, respectively) and then the mixtures incubated for 1 min at 25.0 ± 0.2 °C.

Electron Paramagnetic Resonance Spectroscopy. Analysis of the spin adduct was performed using a Bruker EMX Plus spectrophotometer (Rheinstetten, Germany) operating at X-band, with a magnetic center field of 3473 G, magnetic field sweep of 50 G, microwave frequency of ~9.76 GHz, microwave power of 1 mW, and modulation amplitude of 1 G using a cylindrical ER4103TM cavity and quartz capillary sample cell (ID 0.75 mm, Wilmad Glass, Buena, NJ, U.S.).

Identification of Oxidation Products Derived from Prenylflavonoids and Nonconjugated Unsaturated Fatty Acid Methyl Esters by Oxidation with HER. The oxidation products of prenylated flavonoids XN and IXN generated by the reaction with HER were probed by UHPLC-HESI-II-LTQ Orbitrap Velos FT-MS (Thermo Scientific Co., Bremen, Germany). The reactions were initiated by adding 100 μL of H_2O_2 (59.0×10^{-3} mol L^{-1}) in an argon-saturated ethanol solution containing 80 μL of $FeCl_2{\cdot}4H_2O$ aqueous solution at pH 4.5 (2.0×10^{-3} mol L^{-1}) and substrate (9.8×10^{-5} mol L^{-1} XN; 1.1×10^{-4} mol L^{-1} IXN). After 1 min of reaction at 25.0 ± 0.2 °C, the final reaction solutions were analyzed by ultra-performance liquid chromatography (UPLC) hyphenated to the LTQ Orbitrap Velos mass spectrometer.

To determine the oxidation products formed from the reaction between nonconjugated unsaturated fatty acid methyl esters and HER, we employed methyl linoleate (1.0×10^{-4} mol L^{-1}) as a model compound, and the reaction was carried out as described above for prenylflavonoids. The oxidation products were tentatively identified as assigned by the accurate ultra-high-

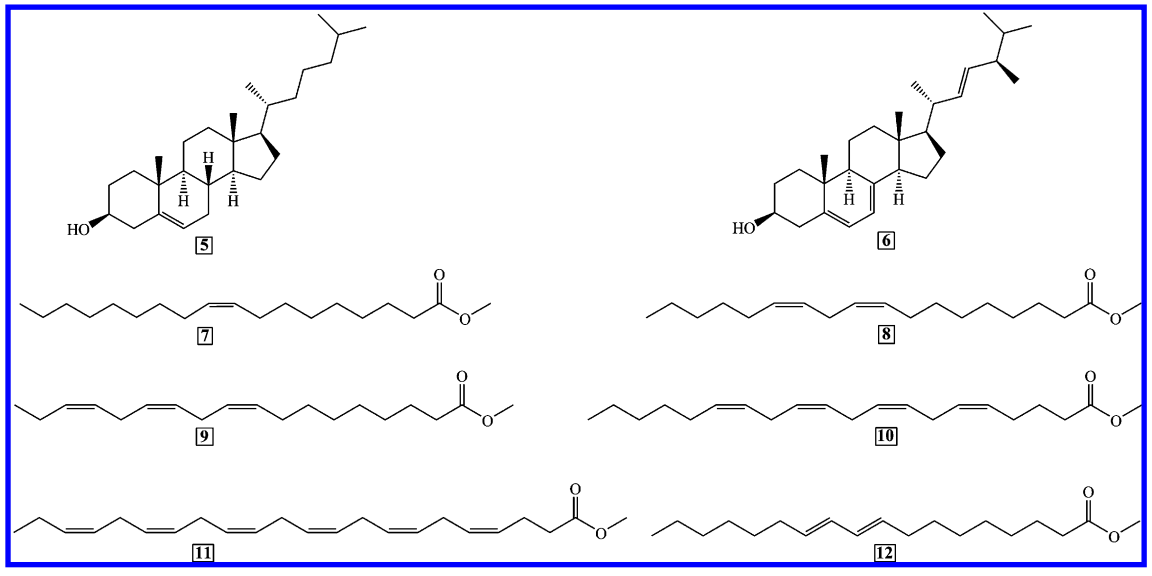

Figure 2. Chemical structures of cholesterol (**5**), ergosterol (**6**), methyl oleate (**7**), methyl linoleate (**8**), methyl linolenate (**9**), methyl arachidonate (**10**), DHA (**11**), and CLA (**12**).

dx.doi.org/10.1021/jp509125b | *J. Phys. Chem. B* 2014, 118, 14278−14287

Table 1. Apparent Second-Order Rate Constants for the Reaction of Prenylflavonoids with HER[a] and Electronic Properties As Calculated by the DFT (6-33++g(2d,2p) Basis Set) Method for the Prenylflavonoids Xanthohumol (XN), Isoxanthohumol (IXN), 6-Prenylnaringenin (6-PN), and 8-Prenylnaringenin (8-PN)

		XN	IXN	6-PN	8-PN
k_{app} ($\times 10^9$ L mol^{-1} s^{-1})		3.6 ± 0.1	1.8 ± 0.1	1.5 ± 0.2	1.7 ± 0.1
IP (kJ mol^{-1})		551	563	574	568
BDE (kJ mol^{-1})	C—H_{prenyl}	307	308	323	309
	O—$H_{(2')}$[b]	380			
	O—$H_{(4)}$[b]	336			
	O—$H_{(7)}$[b]		352	362	361
	O—$H_{(5)}$[b]			379	382
	O—$H_{(4')}$[b]	367	336	347	348

[a]Reactions were carried out in argon-saturated ethanol solutions at 25.0 ± 0.2 °C. [b]As indicated in Figure 1.

performance liquid chromotagraphy (UHPLC) resolution mass spectrometer.

UHPLC-HESI-II-LTQ Orbitrap Velos FT-MS. UHPLC-HESI-II-FT-MS analyses were carried out using a Thermo Scientific UHPLC model Scientific Accela 1250 system with an Accela LC CombiPAL auto sampler injector with a sample loop of 20 μL. Compounds were separated using a Hypersil Gold C-18 reverse phase column (1.9 μm; 50 × 2.1 mm). The mobile phase (flow rate = 0.3 mL min^{-1}) used for the chromatographic separation of the reaction products derived from prenylated flavonoids comprised a linear gradient of a mixture of solvents A (water/formic acid 99.9:0.1, v/v) and B (acetonitrile/formic acid 99.9:0.1, v/v). The eluting gradient of B in A was employed as follows: 0−2 min, 0−10% B in A; 2−5 min, 10−20% B in A; 5−20 min, 20−45% B in A; 20−23 min, 45−55% B in A; 23−25 min, 55−90% B in A; 25−27 min, 90−90% B in A; and 27−30 min, 90−0% B in A. The mobile phase (flow rate = 0.3 mL min^{-1}) used for the chromatographic separation of oxidation products from methyl linoleate comprised a linear elution gradient of a mixture of solvents A (water/formic acid 99.9:0.1, v/v) and B (methanol/formic acid 99.9:0.1, v/v) as follows: 0−3 min, 40−40% B in A; 3−8 min, 40−60% B in A; 8−13 min, 60−75% B in A; 13−20 min, 75−85% B in A; and 20−30 min, 85−85% B in A. The mass spectra were collected in the negative and positive ion modes to identify compounds derived from prenylflavonoids and methyl linoleate, respectively, using an ultra-high-resolution and accurate mass spectrometer LTQ Orbitrap Velos FT-MS equipped with a heated electrospray ionization interface (HESI-II). General HESI conditions were as follows: spray voltage, 3100 V; ion transfer tube temperature, 350 °C; vaporizer temperature, 350 °C; sheath gas pressure, 35 psi; auxiliary gas flow, 10 au; and N_2 gas consumption, 8 L min^{-1}.

Cyclic Voltammetry of Ergosterol and Methyl Ester of Conjugated (9*E*,11*E*)-Linoleic Acid (CLA). Cyclic voltammetry of ergosterol and CLA was carried out using a PAR 264A potentiostat and two platinum wires as working and auxiliary electrodes, employing the couple ferrocene/ferrocenium (Fe^+/Fe) as an internal reference. The compounds (2.0×10^{-3} mol L^{-1} ergosterol; 5.0×10^{-3} mol L^{-1} CLA) were dissolved in a supporting electrolyte solution of tetrabutylammonium perchlorate (0.1 mol L^{-1} in acetonitrile), and the solutions were degassed with high-purity argon before taking measurements. The scan rate was 100 mV s^{-1}, and the electrochemical cell was thermostated at 25.0 ± 0.2 °C. The measured potentials are reported against the normal hydrogen electrode (NHE) using E^0 = +630 mV versus NHE for the couple Fe^+/Fe in acetonitrile.[12]

Computational Methods. All calculations were performed with the Gaussian 09 (G09) program package,[13] C.01 edition, employing the DFT method with Becke's three-parameter hybrid functional[14] and Lee−Yang−Parr's gradient corrected correlation functional (B3LYP) (UB3LYP for the radical species).[15] The 6-31 G basis set[16] was used for optimization of ground-state geometries. The dielectric constant of the ethanol solvent was included in the calculations through the PCM model. SCF-tight convergence criteria were used in all optimizations. For bond dissociation enthalpy (BDE) and ionization potential (IP) calculations, single point energies (SPEs) were carried out using the 6-311++G(2d,2p) set. Thermodynamic correction terms (at 298 K) were obtained through the calculation of vibrational modes (B3LYP/6-311++G(2d,2p)), including the zero-point vibrational energy. BDEs were calculated according to the formula BDE = $H_r + H_H - H$, where H_r is the enthalpy of the radical generated by hydrogen atom abstraction, H_H is the enthalpy of the hydrogen atom, and H is the enthalpy of the precursor molecule. The enthalpy of the hydrogen atom used in the BDE calculation was −0.499897 hartree at this level of theory. IPs were calculated according to the equation IP = $E_{R^+} - E$, where E_{R^+} is the energy of the cation radical generated after electron transfer and E is the energy of the precursor molecule.[17] Computations were performed through the facilities of the Shared Hierarchical Academic Research Computing Network (SHARCNET: www.sharcnet.ca) in Ontario, Canada.

3. RESULTS AND DISCUSSION

Competitive Kinetic Studies. Reactivity of the investigated compounds toward HER was evaluated by determining apparent second-order rate constants for the reactions by means of a competitive kinetic approach.[18,19] Decreases in the spin adduct HER/4-POBN signal intensity resulting from inhibition of spin adduct formation were monitored by EPR spectroscopy as a function of increasing concentration of the substrate (Figure S1, Supporting Information). The EPR spectrum of the spin adduct HER/4-POBN is characterized by a triplet of doublets presenting a nitrogen hyperfine coupling constant of 15.6 G and a hydrogen superhyperfine coupling constant of 2.6 G, which are in agreement with the literature.[20] Thus, from the linear regression fit obtained for the plot of $(F/(1-F))(3.1 \times 10^7)$[4-POBN] versus the concentration of the substrate (Figure S2, Supporting Information), the apparent second-order rate constants were calculated from the slope of the linear dependence, as established by eq 1

$$\left(\frac{F}{1-F}\right)(3.1 \times 10^7)[\text{4-POBN}] = k_2[\text{substrate}] \quad (1)$$

where F represents the percent inhibition for spin adduct formation, 3.1×10^7 (L mol^{-1} s^{-1})[21] is the second-order rate

dx.doi.org/10.1021/jp509125b | J. Phys. Chem. B 2014, 118, 14278−14287

constant of the reaction between the 1-hydroxyethyl radical and the spin trap 4-POBN, and [4-POBN] and [substrate] refer to the concentrations of the spin trap and the substrate employed in the reaction mixtures, respectively.

The apparent second-order rate constants for the reactions involving prenylated flavonoids with HER are collected in Table 1. The orders of magnitude of the observed apparent second-order rate constants for the reactions involving prenylated flavonoids (10^9 L mol^{-1} s^{-1}) are close to the diffusion limit in aqueous medium ($\sim 10^{10}$ L mol^{-1} s^{-1}) and express high reactivity for the thermal oxidation of these compounds promoted by HER. In this way, XN proved to be the most reactive species with an apparent second-order rate constant of $k_2 = (3.6 \pm 0.1) \times 10^9$ L mol^{-1} s^{-1}, whereas similar values ($p = 0.05$) were verified for the apparent rate constants obtained for the reactions involving prenylated flavanones IXN, 6-PN, and 8-PN, which display apparent second-order rate constants of $(1.8 \pm 0.1) \times 10^9$, $(1.5 \pm 0.2) \times 10^9$, and $(1.7 \pm 0.1) \times 10^9$ L mol^{-1} s^{-1}, respectively.

The reactivity of some flavonoids toward HER was previously investigated by Marfak et al.[22] as probed by time-resolved γ-radiolysis techniques; no reaction was observed between the radical and naringenin, the nonprenylated precursor of 6- and 8-PN. By association of the chemical structures of naringenin and prenylated flavanones 6- and 8-PN, it is reasonable to infer that the possible reactive site of prenylflavanones is the prenyl side chain. This is in agreement with the literature, which has suggested that the allylic hydrogen atom present in the prenyl side chain is the reactive site for reactions involving beer bitter acids and HER.[11,23] On the other hand, these results do not justify the enhanced reactivity observed for XN, which most likely has a different, additional reactive site.

Aiming to provide a better understanding of the reaction mechanism between prenylated flavonoids and HER, particularly as it relates to the enhanced reactivity of XN, we calculated their electronic and structural properties by the density functional theory (DFT) method. The data obtained by ab initio DFT calculations are shown in Table 1. Via simple evaluation of the energy values at the highest-occupied molecular orbital (E_{HOMO}) and the ionization potential (IP), it is clear that these parameters cannot explain the enhanced reactivity observed for XN.

Moreover, to compare the IP values with the respective bond dissociation enthalpies (BDEs) collected for the bisallylic C—H_{prenyl} and O—H bonds, we verified that the IP values were at least 169 kJ mol^{-1} higher than the BDE values; hence, these data may suggest that the investigated reaction is governed by hydrogen atom transfer (HAT) from the prenylated flavonoids to the radical rather than by electron transfer (ET). The lower BDE value obtained for the C—H_{prenyl} bond compared to the BDE values for the phenolic O—H bond indicates that the reaction is initiated by bisallylic hydrogen atom abstraction from prenyl side chains by HER rather than by electron transfer or proton-coupled electron transfer from the phenolic O—H group. However, the BDEs obtained for the C—H_{prenyl} bond of the investigated compounds are quite similar to each other and cannot justify the enhanced reactivity observed for XN.

Similar conclusions may be extracted from analysis of the contour plots of the highest-occupied molecular orbitals (HOMOs) verified for the prenylated flavonoids, which are represented here by XN and IXN molecules (Figure 3) because both HOMOs are located primarily on the aromatic ring adjacent to the prenyl side chain. On the other hand, comparing the contour plots of the lowest-unoccupied molecular orbitals (LUMOs) for XN and IXN, we observed that a major orbital

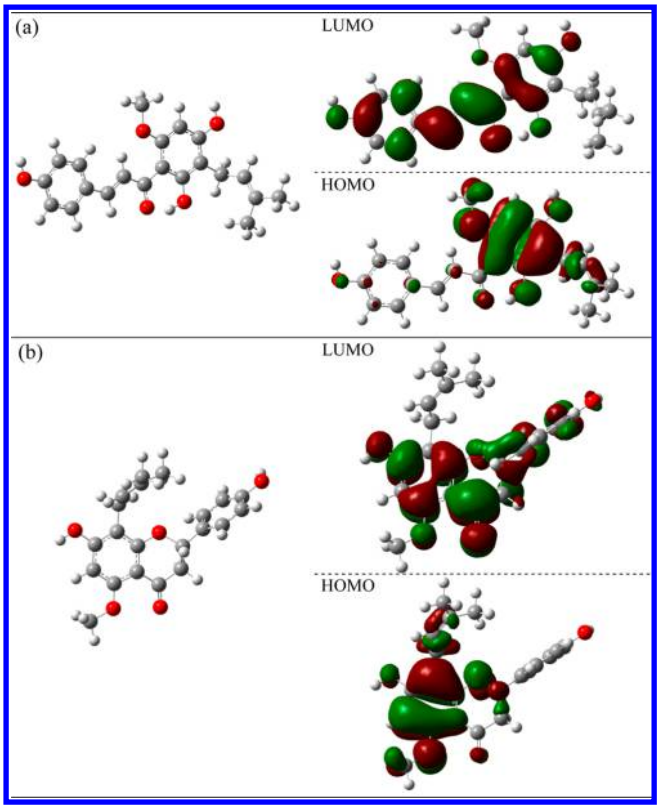

Figure 3. Contour plots of the lowest-unoccupied molecular orbital (LUMO) and highest-occupied molecular orbital (HOMO) of XN (a) and IXN (b).

contribution is located on atoms situated in the α,β-unsaturated carbonyl group of XN, whereas for IXN the referred orbital is mostly centered on atoms belonging to the A, B, and C rings of the molecule. In addition, the calculated energy for the lowest single-occupied molecular orbital (SOMO) for HER is −4.5 eV. The energy difference between the LUMOs of the prenylated flavonoids and the SOMO of the radical is 183 kJ mol^{-1} for XN as calculated by DFT (Figure 4a). Thus, from the present data, we may infer that the α,β-unsaturated carbonyl group of XN is an additional reaction site for HER. Notably, the presence of the carbonyl group adjacent to the double bond acts as an efficient electron-attracting group, lowering the energy of LUMO and facilitating SOMO−LUMO interaction. This strong interaction makes the radical behave like a strong nucleophile, and thus the rate constant of radical addition at the double bond of the α,β-unsaturated carbonyl group is enhanced compared to that of the IXN molecule.

The apparent second-order rate constants obtained for the reactions among HER and unsaturated fatty acid methyl esters and sterols are collected in Table 2. As demonstrated by the apparent rate constants, DHA (C22:6) scavenged HER more efficiently than the other nonconjugated unsaturated fatty acid methyl esters investigated, with $k_2 = (2.7 \pm 0.2) \times 10^7$ L mol^{-1} s^{-1}, whereas no reaction was observed for methyl oleate (C18:1). Indeed, according to our data, reactivity of the nonconjugated unsaturated fatty acids is connected to the number of oxidizable bisallylic methylenic groups in the molecule, because a good linear correlation ($R^2 = 0.989$) was verified for the rates and number of bisallylic hydrogen atoms (Figure S3, Supporting Information). In this way, reactivity of nonconjugated methyl esters of fatty acid seems to be dominated by an entropic factor

dx.doi.org/10.1021/jp509125b | J. Phys. Chem. B 2014, 118, 14278−14287

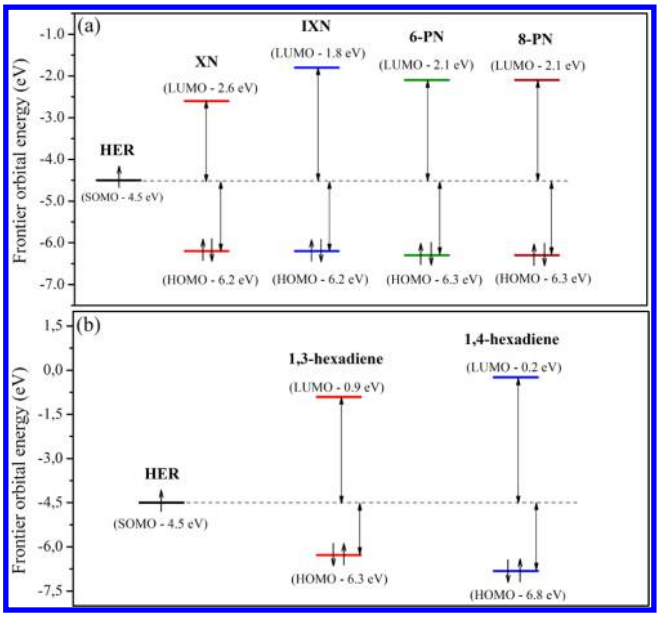

Figure 4. Plot of the energy of the lowest single-occupied molecular orbital (SOMO) for HER versus the energy of the LUMO and HOMO for prenylflavonoids (a) and 1,3- and 1,4-hexadiene (b).

Table 2. Apparent Second-Order Rate Constants for the Reaction of Unsaturated Fatty Acid Methyl Esters and Sterols with HER and Bond Dissociation Enthalpies for the Weakest C—H Bond in the Unsaturated Lipid As Obtained by DFT

substrate	C—H BDE (kJ mol^{-1})	number of bisallylic H atoms	k_{app} ($\times 10^6$ L mol^{-1} s^{-1})[a]
cholesterol	328 (C_7–H)[c]	0	2.7 ± 0.1
ergosterol	296 (C_{14}–H)[d]	0	52 ± 1
methyl oleate	331 (C_8–H)[e]	0	nr[b]
conjugated (9*E*,11*E*) methyl linoleate	311 (C_8–H)[g]	0[c]	13 ± 2
methyl linoleate	294 (C_{11}–H)[e]	2	3.7 ± 0.1
methyl linolenate	293 (C_{11}–H)[e]	4	7.6 ± 0.1
methyl arachidonate	288 (C_{10}–H)[f]	6	15 ± 1
methyl docosahexanoate	267 (C_{12}–H)[f]	10	27 ± 2

[a]Reactions were carried out in argon-saturated ethanol solution at 25.0 ± 0.2 °C. [b]Not reactive (nr). [c]From ref 24. [d]From ref 25. [e]From ref 26. [f]From ref 27. [g]Conjugated double bond.

because the presented rate constants depend strongly on the number of bisallylic hydrogen atoms rather than correlating to BDE values of the bisallylic C—H bonds.

The oxidation potentials of the methyl esters of oleic, linoleic, and linolenic acid are 2.12, 2.06, and 2.05 V, respectively, relative to NHE.[26] The oxidation potentials for CLA and ergosterol were determined experimentally, and the obtained values were 1.95 and 1.40 V, respectively, relative to NHE. Thus, by comparing the oxidation potential for the unsaturated lipids and the reduction potential of HER (E = 0.98 V relative to NHE),[28] we may infer that the ET reaction of the radical with methyl esters of both fatty acids and sterols is thermodynamically unfavorable.

Surprisingly, CLA (C18:2 9*E*,11*E*) was very reactive toward HER, with $k_2 = (1.3 \pm 0.2) \times 10^7$ L mol^{-1} s^{-1}. In fact, this reactivity does not seem to be correlated to the bisallylic HAT or ET reaction. From the frontier orbital energy calculated for the conjugated 1,3-hexadiene and nonconjugated 1,4-hexadiene (Figure 4b), the HOMO energy for the conjugated diene is verified to display a small energy gap (174 kJ mol^{-1}) relative to the radical SOMO, which most likely facilitates the SOMO–HOMO orbital interaction for electrophilic addition of the radical to the conjugated unsaturated system. Thus, according to our results, this orbital interaction confers electrophilic behavior to HER, resulting in its addition at the double bond of the conjugated system.

Concerning the reactivity of sterols toward HER, ergosterol was found to be 19-fold more reactive than cholesterol. Indeed, unsaturated cycloalkenes containing conjugated double bonds have been shown to be more susceptible to oxidation.[27,29] This enhanced reactivity is recognized to be due to conformational effects leading to resonance-stable transition states, which in turn allows for more efficient hydrogen atom abstraction.[29] Additionally, the significant reactivity revealed by cycloalkene sterols functioning as hydrogen atom donors relative to acyclic olefins could be associated with conformational arrangement of the C—H bond at the cyclic structure, conferring maximum frontier orbital overlap between the alkene π bond and the cycloalkane-derived radical.[29] Regarding HER scavenging ability, even though the polyunsaturated fatty acid methyl esters and sterols were shown to be more reactive than the phenolic compounds, like quercetin ($k_2 = 4.0 \times 10^4$ L mol^{-1} s^{-1}),[22] and the polyphenolic compounds containing an α,β-unsaturated carbonyl side chain, such as *p*-coumaric acid ($k_2 = 1.0 \times 10^7$ L mol^{-1} s^{-1}),[11] the rate of oxidation is shown to be higher for prenylflavonoids and thiol-containing substances like glutathione ($k_2 = 7.1 \times 10^8$ L mol^{-1} s^{-1}).[30]

Identification of the Primary Oxidation Products of Prenylflavonoids by Their Reaction with HER. The primary oxidation products resulting from reactions of XN and IXN with HER were identified through analyses of the reaction solutions by UHPLC-HESI-II-LTQ Orbitrap Velos FT-MS. From the total ion chromatogram obtained by the analysis of oxidation products derived from XN (Figure 5a), four primary eluting peaks were found (indicated as A, B, C, and D in the TIC chromatogram); the first three peaks refer to reaction products, whereas peak D is identified as the initial substrate XN. The MS spectra for the recorded eluting peaks (Figure S4, Supporting Information) revealed the presence of a quasi-molecular ion $[M - H]^-$ at m/z 441.4944 for peak A (error of 2.0 ppm as calculated for m/z $[C_{25}H_{30}O_7 - H]^-$ = 441.4935) with retention time (rt) = 18.2 min, which suggests the formation of a compound resulting from the addition of two HER molecules to the substrate. On the other hand, quasi-molecular ions $[M - H]^-$ at m/z 397.4417 and 397.4415 were observed for peaks B and C (error of 1.8 and 1.2 ppm, respectively, as calculated for m/z $[C_{23}H_{26}O_6 - H]^-$ = 397.4410) with rt = 21.0 and 21.7 min, respectively, indicating the formation of two positional isomers arising from covalent linkage of one HER at the XN molecule.

In a recent study, compounds containing a HER molecule added to the prenyl side chain of lupulones were verified to be the primary oxidation products formed by oxidation with HER.[23] In fact, the proposed mechanism for this reaction is that allylic hydrogen atom abstraction from the prenyl side chain of the substrate gives rise to a resonance-stabilized radical, which further reacts with another HER molecule to yield the identified radical addition product.[23] Thus, according to the literature[23] and to our experimental and theoretical data, three possible oxidation products for the reaction mechanism involving XN and HER are proposed, as shown in Scheme 1.

dx.doi.org/10.1021/jp509125b | J. Phys. Chem. B 2014, 118, 14278–14287

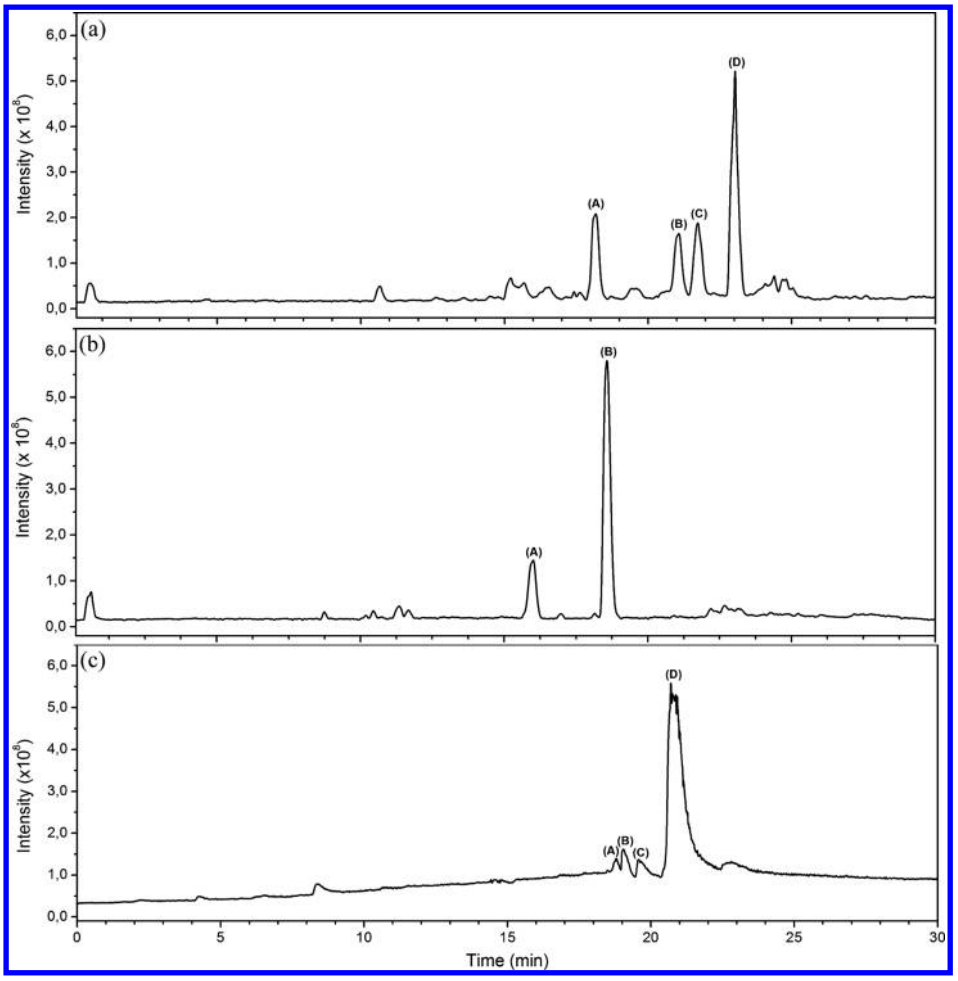

Figure 5. UHPLC-HESI-II-LTQ Orbitrap FT-MS chromatograms of the final compositions obtained from the reactions of XN (a) and IXN (b) with HER, and an UPLC-HESI-II-LTQ Orbitrap FT-MS chromatogram of the final composition obtained from the reaction of methyl linoleate with HER (c). Reactions were carried out in an argon-saturated alcoholic solution (ethanol) at 25.0 ± 0.2 °C. Analysis was performed after 1 min of reaction operating in the negative (a and b) and positive (c) ion detection mode using an electrospray ion source.

The first pathway is initiated by bisallylic hydrogen atom transfer from XN (**1**) to HER, yielding a tertiary resonance-stabilized radical. Further reaction of this tertiary resonance-stabilized radical with HER yields one of the identified positional isomers (**13**). The reaction may be followed by subsequent carbon radical 1,4-addition to the α,β-unsaturated carbonyl group of XN to yield an alkoxyl radical that may further acquire a hydrogen atom from oxidizable species present in the reaction medium, such as XN, to give rise to the oxidation product formed from covalent linkage of two HER molecules at the initial substrate (**14**).

The second pathway considers the 1,4-addition reaction of HER to XN as the primary step, yielding an alkoxyl radical derived from the initial substrate, which then acquires a hydrogen atom from an oxidizable species, resulting in the formation of the other identified positional isomer (**15**). Finally, the oxidation product containing two molecules of HER attached to the XN structure (**14**) is formed through bisallylic hydrogen atom abstraction from the derived substrate (**15**) by HER, followed by radical recombination reactions.

According to the proposed mechanisms, the apparent rate constant obtained for the reaction of XN with HER ($(3.6 \pm 0.1) \times 10^9$ L mol^{-1} s^{-1}) may be considered an average of the rate constants for pathways 1 and 2 as indicated in Scheme 1. In general, it is known that the order of magnitude of the reaction rate for allylic hydrogen atom abstraction from a prenyl side chain by HER ranges from 10^8 to 10^9 L mol^{-1} s^{-1}, as previously reported.[11,23] To evaluate the addition reaction between an α,β-unsaturated carbonyl group and the studied radical, we investigated the reactivity of cinnamaldehyde with HER. The apparent second-order rate constant for the radical addition of HER to cinnamaldehyde is $(7.4 \pm 0.3) \times 10^7$ L mol^{-1} s^{-1}, which may be considered to be an estimate of the rate constant for the carbon radical 1,4-addition reaction to the α,β-unsaturated carbonyl group (k_3 and k_4, Scheme 1). As a comparative, the apparent second-order rate constant for the reaction between cinnamic acids and HER is 1.0×10^7 L mol^{-1} s^{-1} for *p*-coumaric acid as reported in the literature.[11] Thus, the major contribution for the observed rate constant for the reaction between XN and HER comes from the bisallylic hydrogen abstraction reaction (k_1, Scheme 1).

The chromatogram (Figure 5b) from the analysis of the reaction mixture containing IXN, ferric ions, and hydrogen peroxide had two primary eluting peaks (A and B); the late eluting peak (B) is substrate IXN, whereas peak A refers to the respective oxidation product. The MS spectrum for peak A (Figure S5, Supporting Information) revealed the presence of a quasi-molecular ion $[M - H]^-$ at m/z 397.4421 (error of 2.8 ppm as calculated for m/z $[C_{23}H_{26}O_6 - H]^-$ = 397.4410) with rt

dx.doi.org/10.1021/jp509125b | J. Phys. Chem. B 2014, 118, 14278−14287

Scheme 1. Proposed Reaction Mechanisms for the Reaction between HER and XN

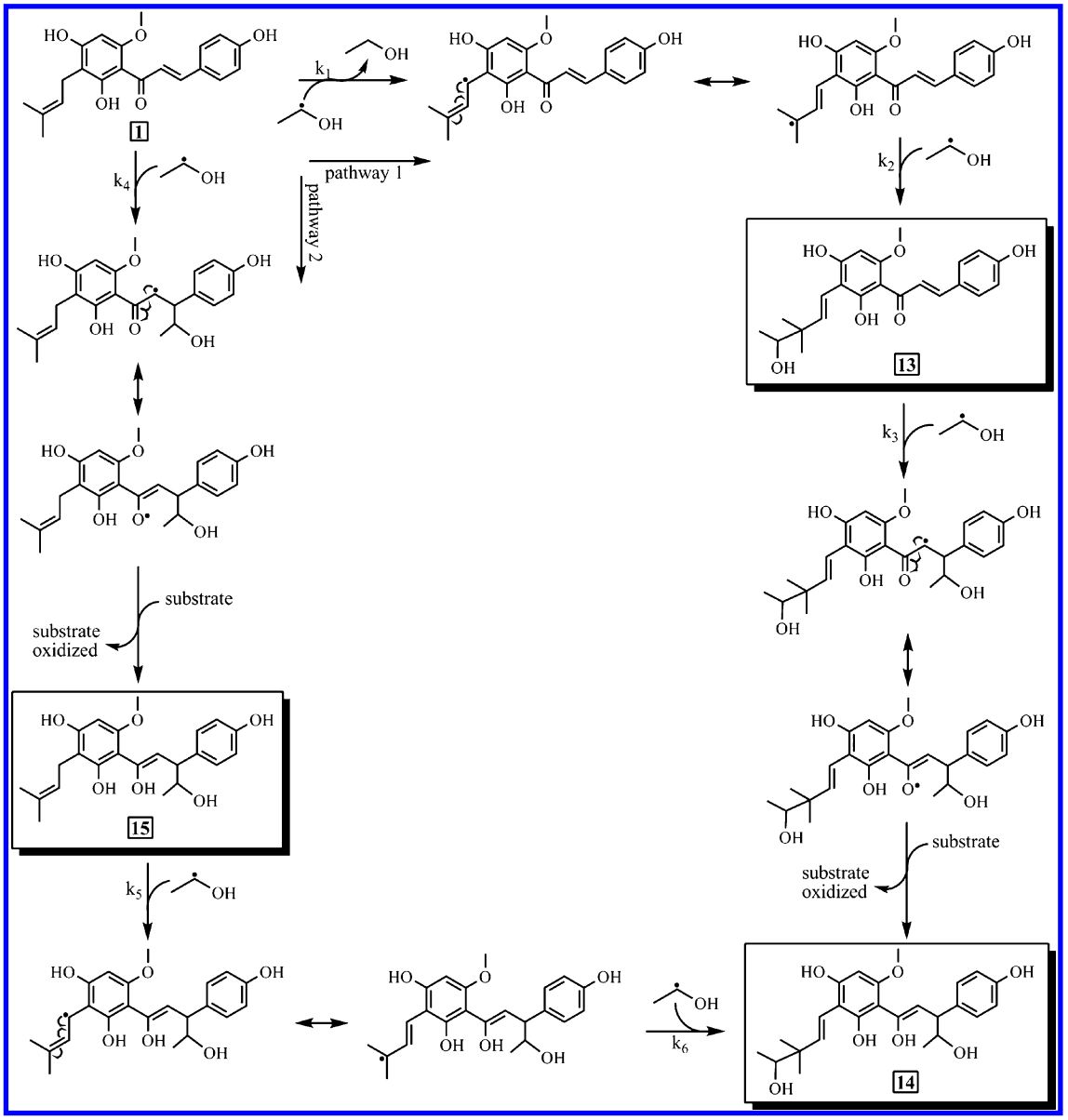

= 16.0 min, suggesting the formation of an IXN oxidative product containing a HER molecule.

From this data, a proposed mechanism for the reaction between IXN and HER is shown in Scheme 2. The reaction is initiated by hydrogen atom abstraction from the prenyl side chain of the substrate (**2**) by HER, yielding a resonance-stabilized radical. The reaction undergoes subsequent radical recombination to yield the oxidized product (**16**). In this case, the major contribution for the apparent second-order rate constant obtained for the investigated reaction is k_1 as indicated in Scheme 2. The oxidation products derived from XN (tentatively assigned as **13**, **14**, and **15**) and IXN (tentatively assigned as **16**) have not been reported previously in the literature, and they may represent novel oxidation derivatives of prenylated flavonoids.

Identification of Primary Oxidation Products of Non-conjugated Unsaturated Fatty Acid Methyl Esters by Their Reaction with HER. The UHPLC-HESI-II-LTQ Orbitrap Velos FT-MS chromatogram revealed the presence of four eluting peaks; the first three peaks (A, B, and C with rt = 18.8, 19.0, and 19.6 min, respectively) refer to the reaction products, and peak D (rt = 20.9 min) is identified as the precursor unsaturated fatty acid methyl ester (Figure 5c). The eluting peaks relating to the oxidation products revealed similar MS spectra (Figure S6, Supporting Information), with a quasi-molecular ion $[M + H]^+$ at m/z 311.4787 (error of −2.2 ppm as calculated for m/z $[C_{19}H_{34}O_3 + H]^+$ = 311.4794), suggesting the formation of hydroxide derivatives of methyl linoleate.

Several studies have reported mechanisms involved in the oxidation of unsaturated fatty acids, which are based on the formation of hydroperoxides, cyclic peroxides, and hydroxide derivatives.[31−33] Thus, according to our experimental results and those in the literature, a reaction mechanism involving methyl linoleate and HER has been proposed as shown in Scheme 3. The reaction may be initiated by bisallylic hydrogen atom abstraction from the unsaturated fatty acid methyl ester (**8**) by HER to yield three intermediate carbon-centered resonance-stabilized radicals, which react with the hydroxyl radical to yield hydroxylated methyl linoleate derivatives **17**, **18**, and **19**.

dx.doi.org/10.1021/jp509125b | J. Phys. Chem. B 2014, 118, 14278−14287

Scheme 2. Proposed Reaction Mechanism for the Reaction between HER and IXN

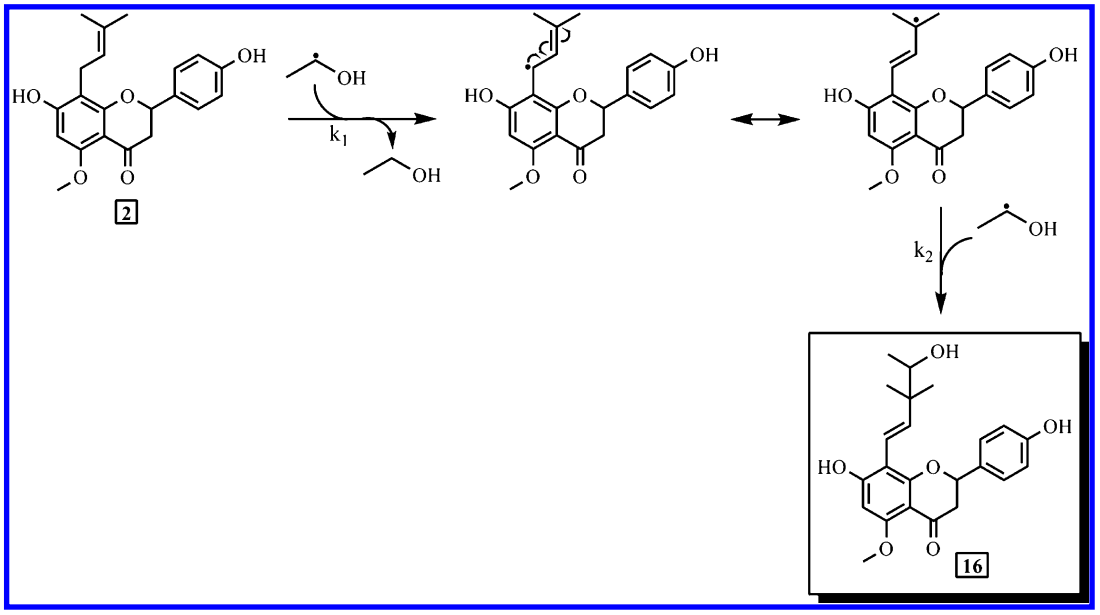

Scheme 3. Proposed Reaction Mechanism for the Reaction between HER and Methyl Linoleate in Anaerobic Medium

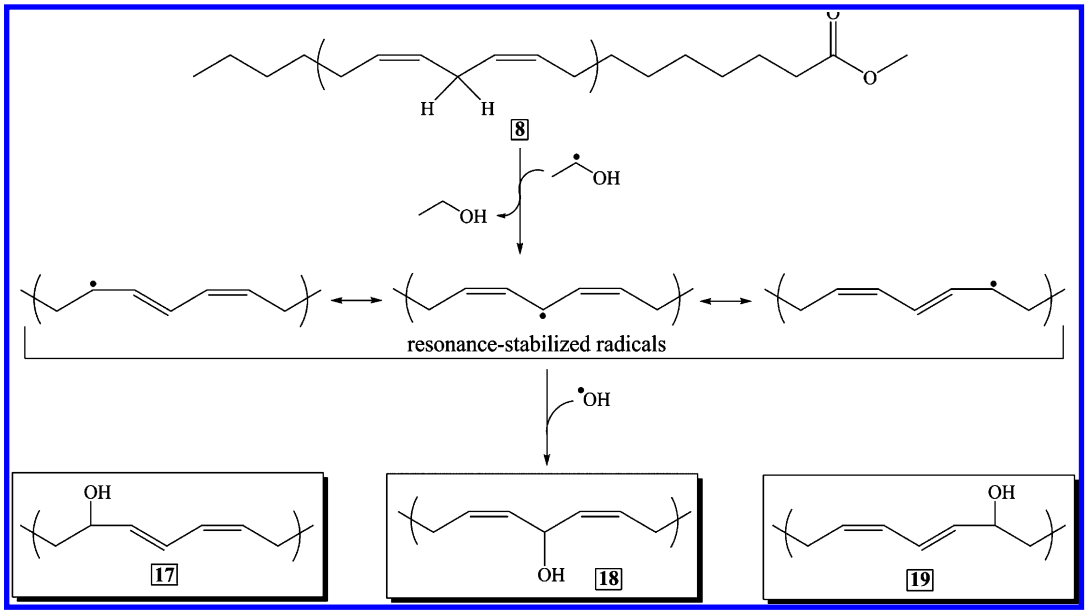

Biological Relevance. Ethanol is well-known to be metabolized in the human body by various oxidative and nonoxidative pathways. The main oxidative pathways for ethanol metabolism in the liver primary involve the enzymes aldehyde dehydrogenase, alcohol dehydrogenase, microsomal cytochrome P450, and catalase. The metabolism of ethanol to hydroxyethyl radicals, relevant at high ethanol concentrations and induced by chronic alcohol consumption, occurs in the centrilobular region of the liver by the microsomal cytochrome P450 pathway at the cell's network membrane.[34,35] Under these conditions, a distribution between the aqueous and lipid compartments in the cell becomes relevant. In that view, the steady-state mass balance for any target species (X) may be described by eq 2

$$(1 - V)R_{aq} + VR_{LH} = 0 \quad (2)$$

where V is the volume fraction of the lipid phase in the cell (~3%)[36] and R_{aq} and R_{LH} are the net rate of formation of the target species in the aqueous and lipid phase, respectively. Another important aspect to be taken into account is the distribution constant for X species in the aqueous/lipid phase, which may be described by $K_D = [X]_{LH}/[X]_{aq}$ if a high mass transfer rate constant is considered, to ensure that the species distribution is close to the equilibrium value.

On the basis of the assumptions listed above and reactions that may produce or consume HER in the cell (Scheme 4), the net rates of HER formation in the aqueous and lipid phase are

$$R_{aq} = f[\text{HER}] - [\text{HER}](k_1[\text{GSH}] + k_2[\text{6-PN}] + k_3[\text{O}_2]) \quad (3)$$

$$R_{LH} = k_{CYP}[\text{EtOH}] - [\text{HER}](k_2[\text{6-PN}] + k_3[\text{O}_2] + k_4[\text{LH}]) \quad (4)$$

dx.doi.org/10.1021/jp509125b | J. Phys. Chem. B 2014, 118, 14278−14287

Scheme 4. Model Used To Describe the Reactions Involved in the Production and Consumption of 1-Hydroxyethyl Radical in the Cell Network

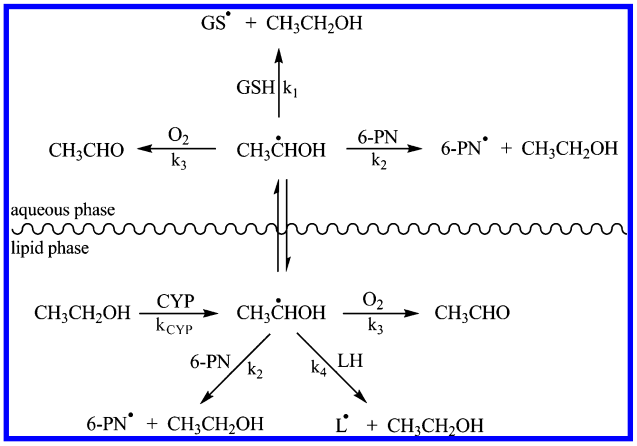

respectively, where f is the fraction of HER produced in the cell membrane network that may diffuse to the aqueous phase (cytosol), and k_{CYP} is the rate constant for formation of HER as catalyzed by microsomal cytochrome P450.

From eqs 3 and 4, we may write the following expression for HER concentration

$$[\mathrm{HER}] = ([\mathrm{HER}](1 - V)f + V(1 - f)k_{CYP}[\mathrm{EtOH}]) / (\{(1 - V)(k_1[\mathrm{GSH}] + k_2[\text{6-PN}] + k_3[\mathrm{O_2}]) [\mathrm{HER}] + V(k_2[\text{6-PN}] + k_3[\mathrm{O_2}] + k_4[\mathrm{LH}])) \quad (5)$$

Equation 5 can be further simplified assuming $f[\mathrm{HER}]$ is very small, and $V(1 - f)k_{CYP}[\mathrm{EtOH}] \gg (1 - V)f$. The terms describing the fraction of HER that diffused to the aqueous phase in the numerator and the aqueous consumption of HER in the denominator may be considered negligible. Thus, the final expression for HER concentration is

$$[\mathrm{HER}] = \frac{k_{CYP}[\mathrm{EtOH}]}{k_2[\text{6-PN}] + k_3[\mathrm{O_2}] + k_4[\mathrm{LH}]} \quad (6)$$

Assuming an oxygen concentration in the centrilobular region of liver tissue during ethanol consumption around 1×10^{-5} mol L^{-1} ($K_{D(O_2)} = 3$),[37] a 6-PN concentration of 2×10^{-5} mol L^{-1} ($K_{D(6\text{-PN})} = 3.7$),[38] and a polyunsaturated lipid content of 2×10^{-2} mol L^{-1},[39] we may calculate individual contributions for the lipid phase sink of HER from eq 6. The major sink for HER under these conditions is the reaction with polyunsaturated lipids, which accounts for ~87% of the denominator in eq 6, followed by oxygen and 6-PN accounting for 8.7% and 3.5%, respectively.

4. CONCLUSIONS

The data presented here provide strong evidence that polyunsaturated fatty acids are reactive oxidizable species for carbon-centered hydroxyalkyl radical-mediated oxidation in biological settings, further emphasizing the critical role of radical-mediated oxidation in the pathogenesis of fatty liver diseases. Prenylated phenolic compounds are shown to be potential natural antioxidants for protecting biomolecules and sensitive structures against oxidation promoted by carbon-centered hydroxyalkyl radicals reacting either by hydrogen atom transfer yielding the reduced radical and a stable phenoxyl radical or by radical addition to the α,β-unsaturated carbonyl group to yield a stable radical adduct.

■ ASSOCIATED CONTENT

Supporting Information

Experimental EPR spectra of the HER/4-POBN spin adduct, plot of $(F/(1 - F))k_2[\text{4-POBN}]$ versus the concentration of IXN and methyl linoleate, plot of the apparent second-order rate constants for the reaction of polyunsaturated fatty acid methyl esters with HER versus the number of oxidizable bisallylic methylenic hydrogen atoms, and mass spectra recorded for the eluting peaks indicated in Figure 5a–c. This material is available free of charge via the Internet at http://pubs.acs.org.

■ AUTHOR INFORMATION

Corresponding Author

*E-mail: drcardoso@iqsc.usp.br. Phone: +55 16 33 73 99 76.

Notes

The authors declare no competing financial interest.

■ ACKNOWLEDGMENTS

This research is part of the bilateral Brazilian/Danish Food Science Research Program "BEAM - Bread and Meat for the Future" supported by FAPESP (Grant 2011/51555-7) to D.R.C. and by the Danish Research Council for Strategic Research (Grant 11-116064). D.R.C. thanks the Brazilian National Research Council CNPq for research fellowship 306956/2012-8. N.E.C.A. thanks FAPESP for the Ph.D. fellowship (2011/09273-4) and EMU (2009/54040). Prof. A. B. P. Lever (Department of Chemistry, York University, Toronto, Canada) is acknowledged for granting computational time at the Shared Hierarchical Academic Research Computing Network (SHARCNET: www.sharcnet.ca) in Ontario, Canada.

■ ABBREVIATIONS

BDE, bond dissociation enthalpy; CLA, methyl ester of conjugated (9*E*,11*E*)-linoleic acid; DFT, density functional theory; DHA, methyl ester of docosahexaenoic acid; EPR, electron paramagnetic resonance; ET, electron transfer; G09, Gaussian 09; HAT, hydrogen atom transfer; HER, 1-hydroxyethyl radical; HOMO, highest-occupied molecular orbital; IP, ionization potential; IXN, isoxanthohumol; LUMO, lowest-unoccupied molecular orbital; MS, mass spectrometry; NHE, normal hydrogen electrode; 6-PN, 6-prenylnaringenin; 8-PN, 8-prenylnaringenin; 4-POBN, α-(4-pyridyl-1-oxide)-*N*-*tert*-butylnitrone; SPEs, single point energies; SOMO, single-occupied molecular orbital; UHPLC, ultra-high-performance liquid chromatography; XN, xanthohumol

■ REFERENCES

(1) Nordmann, R.; Riviere, C.; Rouach, H. Implication of Free Radical Mechanisms in Ethanol-Induced Cellular Injury. *Free Radical Biol. Med.* **1992**, *12*, 219–240.

(2) Cederbaum, A. I. Oxygen Radical Generation by Microsomes: Role of Iron and Implications for Alcohol Metabolism and Toxicity. *Free Radical Biol. Med.* **1989**, *7*, 559–567.

(3) Reinke, L. A.; Moore, D. R.; McCay, P. B. Mechanisms for Metabolism of Ethanol to 1-Hydroxyethyl Radicals in Rat Liver Microsomes. *Arch. Biochem. Biophys.* **1997**, *348*, 9–14.

(4) Reinke, L. A. Spin Trapping Evidence for Alcohol-Associated Exudative Stress. *Free Radical Biol. Med.* **2002**, *32*, 953–957.

(5) Poli, G. Liver Damage Due to Free Radicals. *Br. Med. Bull.* **1993**, *49*, 604–620.

(6) Videla, L. A.; Valenzula, A. Alcohol Ingestion, Liver Glutathione and Lipoperoxidation: Metabolic Interrelationships and Pathological Implications. *Life Sci.* **1982**, *31*, 2395−2407.
(7) Stoyanovsky, D. A.; Wu, D.; Cederbaum, A. I. Interaction of 1-Hydroxyethyl Radical with Glutathione, Ascorbic Acid and α-Tocopherol. *Free Radical Biol. Med.* **1998**, *24*, 132−138.
(8) Scalbert, A.; Manach, C.; Morand, C.; Rémésy, C.; Jiménez, L. Dietary Polyphenols and the Prevention of Diseases. *Crit. Rev. Food Sci. Nutr.* **2005**, *45*, 287−306.
(9) Pinto, C.; Duque, A. L.; Rodríguez-Galdón, B.; Cestero, J. J.; Macías, P. Xanthohumol Prevents Carbon Tetrachloride-Induced Acute Liver Injury in Rats. *Food Chem. Toxicol.* **2012**, *50*, 3405−3412.
(10) Mukai, R.; Fujikura, Y.; Murota, K.; Uehara, M.; Minekawa, S.; Matsui, N.; Kawamura, T.; Nemoto, H.; Terao, J. Prenylation Enhances Quercetin Uptake and Reduces Efflux in Caco-2 Cells and Enhances Tissue Accumulation in Mice Fed Long-Term. *J. Nutr.* **2013**, *143*, 1558−1564.
(11) de Almeida, N. E. C.; Homem-de-Mello, P.; De Keukeleire, D.; Cardoso, D. R. Reactivity of Beer Bitter Acids Toward the 1-Hydroxyethyl Radical as Probed by Spin-Trapping Electron Paramagnetic Resonance (EPR) and Electrospray Ionization-Tandem Mass Spectrometry (ESI-MS/MS). *J. Agric. Food Chem.* **2011**, *59*, 4183−4191.
(12) Pavlishchuk, V. V.; Addison, A. W. Conversion Constants for Redox Potentials Measured Versus Different Reference Electrodes in Acetonitrile Solutions at 25 °C. *Inorg. Chim. Acta* **2000**, *298*, 97−102.
(13) Frisch, M. J.; Trucks, G. W.; Schlegel, H. B.; Scuseria, G. E.; Robb, M. A.; Cheeseman, J. R.; Montgomery, J. A., Jr.; Vreven, T.; Kudin, K. N.; Burant, J. C.; et al. *Gaussian 03*, revision D.01; Gaussian Inc.: Wallingford, CT, 2004.
(14) Becke, A. D. Density-Functional Thermochemistry. III. The Role of Exact Exchange. *J. Chem. Phys.* **1993**, *98*, 5648−5652.
(15) Lee, C.; Yang, W.; Parr, R. G. Development of the Colle-Salvetti Correlation-Energy Formula Into a Functional of the Electron Density. *Phys. Rev. B: Condens. Matter Mater. Phys.* **1988**, *37*, 785−789.
(16) Hay, P. J.; Wadt, W. R. Ab Initio Effective Core Potentials for Molecular Calculations. Potentials for K to Au Including the Outermost Core Orbitals. *J. Chem. Phys.* **1985**, *82*, 270−283.
(17) Nenadis, N.; Sigalas, M. P. A DFT Study on the Radical Scavenging Potential of Selected Natural 3′,4′-Dihydroxy Aurones. *Food Res. Int.* **2011**, *44*, 114−120.
(18) Ogusucu, R.; Rettori, D.; Muchoz, D. C.; Soares Netto, L. E.; Ohara, A. Reactions of Yeast Thioredoxin Peroxidases I and II with Hydrogen Peroxide and Peroxynitrite: Rate Constants by Competitive Kinetics. *Free Radical Biol. Med.* **2007**, *42*, 326−334.
(19) Winterbourn, C. C. The Ability of Scavengers to Distinguish $OH^{\bullet}$ Production in the Iron-Catalyzed Haber-Weiss Reaction: Comparison of Four Assays for $OH^{\bullet}$. *Free Radical Biol. Med.* **1987**, *3*, 33−39.
(20) Andersen, M. L.; Skibsted, L. H. Electron Spin Resonance Spin Trapping Identification of Radicals Formed During Aerobic Forced Aging of Beer. *J. Agric. Food Chem.* **1998**, *46*, 1272−1275.
(21) Pou, S.; Ramos, C. L.; Gladwell, T.; Renks, E.; Centra, M.; Young, D.; Cahen, M. S.; Rosen, G. M. A Kinetic Approach to the Selection of a Sensitive Spin Trapping System for the Detection of Hydroxyl Radical. *Anal. Biochem.* **1994**, *217*, 76−83.
(22) Marfak, A.; Trouillas, P.; Allais, D. P.; Calliste, C. A.; Cook-Moreau, J.; Duroux, J. Reactivity of Flavonoids with 1-Hydroxyethyl Radical: A γ-Radiolysis Study. *Biochim. Biophys. Acta, Gen. Subj.* **2004**, *1670*, 28−39.
(23) de Almeida, N. E. C.; do Nascimento, E. S. P.; Cardoso, D. R. On the Reaction of Lupulones, Hops β-Acids, with 1-Hydroxyethyl Radical. *J. Agric. Food Chem.* **2012**, *60*, 10649−10656.
(24) Lengyel, J.; Rimarcik, J.; Vaganek, A.; Fedor, J.; Lukes, V.; Klein, E. Oxidation of Sterols: Energetics of C−H and O−H Bond Cleavage. *Food Chem.* **2012**, *133*, 1435−1440.
(25) Agapito, F.; Nunes, P. M.; Cabral, B. J. C.; Santos, R. M. B.; Simoes, J. A. M. Energetics of the Allyl Group. *J. Org. Chem.* **2007**, *72*, 8770−8779.
(26) Huvaere, K.; Cardoso, D. R.; Homem-de-Mello, P.; Westermann, S.; Skibsted, L. H. Light-Induced Oxidation of Unsaturated Lipids as Sensitized by Flavins. *J. Phys. Chem. B* **2010**, *114*, 5583−5593.
(27) Cardoso, R. C.; Scurachio, R. S.; Santos, W. G.; Homem-de-Mello, P.; Skibsted, L. H. Riboflavin-Photosensitized Oxidation is Enhanced by Conjugation in Unsaturated Lipids. *J. Agric. Food Chem.* **2013**, *61*, 2268−2275.
(28) Koppenol, W. H.; Butler, J. Energetics of Interconversion Reactions of Oxyradicals. *Adv. Free Radical Biol. Med.* **1985**, *1*, 91−131.
(29) Xu, L.; Davis, T. A.; Porter, N. A. Rate Constants for Peroxidation of Polyunsaturated Fatty Acids and Sterols in Solution and in Liposomes. *J. Am. Chem. Soc.* **2009**, *131*, 13037−13044.
(30) de Almeida, N. E. C.; Lund, M. N.; Andersen, M. L.; Cardoso, D. R. Beer Thiol-Containing Compounds and Redox Stability: Kinetic Study of 1-Hydroxyethyl Radical Scavenging Ability. *J. Agric. Food Chem.* **2013**, *61*, 9444−9452.
(31) Porter, N. A.; Caldwell, S. E.; Mills, K. A. Mechanisms of Free Radical Oxidation of Unsaturated Lipids. *Lipids* **1995**, *30*, 277−290.
(32) Ying, H.; Porter, N. A. New Insights Regarding the Autoxidation of Polyunsaturated Fatty Acids. *Antioxid. Redox Signaling* **2005**, *7*, 170−184.
(33) Brash, A. R. Autoxidation of Methyl Linoleate: Identification of the Bis-Allylic 11-Hydroperoxide. *Lipids* **2000**, *35*, 947−952.
(34) Koop, D. R. Oxidative and Reductive Metabolism by Cytochrome P450 2E1. *FASEB J.* **1992**, *6*, 724−730.
(35) Lieber, C. S. The Discovery of the Microsomal Ethanol Oxidizing System and its Physiologic and Pathological Role. *Drug Metab. Rev.* **2004**, *36*, 511−529.
(36) Liu, X.; Miller, M. J. S.; Joshi, M. S.; Thomas, D. D.; Lancaster, J. R. Accelerated Reaction of Nitric Oxide with O_2 within the Hydrophobic Interior of Biological Membranes. *Proc. Natl. Acad. Sci. U.S.A.* **1998**, *95*, 2175−2179.
(37) Lewis, R. S.; Tamir, S.; Deen, W. M. Kinetic Analysis of the Fate of Nitric Oxide Synthesized by Macrophages in Vitro. *J. Biol. Chem.* **1995**, *270*, 29350−29355.
(38) Terao, J.; Mukai, R. Prenylation Modulates the Bioavailability and Bioaccumation of Dietary Flavonoids. *Arch. Biochem. Biophys.* **2014**, *559*, 12−16.
(39) Abbott, S. K.; Else, P. L.; Atkins, T. A.; Hulbert, A. J. Fatty Acid Composition of Membrane Bilayers: Importance of Diet Polyunsaturated Fat Balance. *Biochim. Biophys. Acta* **2012**, *1818*, 1309−1317.